Available online at www.sciencedirect.com
SCIENCE DIRECT®
Polymer 46 (2005) 7644–7651
polymer
www.elsevier.com/locate/polymer

Study of a skin-core type of crystallinity distribution within polyethylene specimen crystallized under high pressure

Jie Kong*, Xiaodong Fan, Wenqiang Qiao, Yunchuan Xie, Qinfa Si, Yusheng Tang

Department of Applied Chemistry, School of Science, Northwestern Polytechnical University, Xi' an 710072, People's Republic of China

Received 15 October 2004; received in revised form 18 March 2005; accepted 10 April 2005
Available online 12 July 2005

Abstract

The regularity of 'skin-core' type of crystallinity distribution within the polyethylene cylindrical specimen crystallized under high pressure was investigated via modulated differential scanning calorimeter (MDSC), wide angle X-ray diffraction meter (WAXD), dynamic mechanical analyzer (DMA) and scanning electron microscope (SEM). The relationship between the gradient of high pressure stress field and the 'skin-core' structure of polyethylene was also established. The results indicate that there exists a distinguished difference of crystallinity, morphology and dynamical mechanical properties between skin layer and core region within the cylindrical specimen crystallized under 650 MPa pressure. The measurement data of the non-reversible heat flow of MDSC and WAXD for both skin layer and core region are in accordance with that marked difference. According to the law of stress decay of high pressure stress field and the high pressure crystallization theory of polymers, it was found that the uneven distribution of high pressure stress field, especially, the high pressure decay effect at the edge of plunger and cylindrical channel of the mold is proposed as the principal factor to the formation of the 'skin-core' type of crystallinity distribution within the polyethylene cylindrical specimen crystallized under high pressure.

Keywords: Skin-core; High pressure crystallization; Polyethylene

1. Introduction

It is well known that semi-crystalline polymers such as polyethylene (PE), poly (vinylidene fluride) (PVDF), polyamides (PA), poly (ethylene terephthalate) (PET) and poly (ethylene 2,6-naphalate) (PEN) can present extended chain crystals morphology if they are crystallized under high pressure and high temperature [1–4]. Particularly, since Wunderlich et al. revealed the concept of so called the extended chain crystals of linear polyethylene [5,6], a considerable number of studies have been made on the novel crystals and their aggregate state for polyethylene. It was discovered for high pressure crystallized polyethylene that there exist various kinds of crystalline morphologies including extended chain crystal, folded chain crystal, interphase structure, and lobation or spherulite aggregate structure [7,8]. And others novel crystals, such as the granular crystals, rodlike crystals and shish-kebab crystals, were even presented in different locations of the linear polyethylene specimen crystallized under supra-high pressure of 0.7–2.3 GPa [9,10]. This further indicated that the high pressure stress field may have the potential role on the creation of novel crystalline structure for polyethylene.

One of the reasons for the continuous focuses on the extended chain crystals is that the crystals with high tacticity and crystallinity can effectively overcome the influence of structural heterogeneity and viscoelasticity of macromolecular chains on the mechanical properties of materials [11–14]. To date, based on the self-reinforcement theory of polymers, polyethylene film, rod, or sheet products with high strength and high modules have been fabricated by using high pressure injection moulding, or solid deformation process of high pressure crystallized polyethylene [15–17]. During conducting a research project for preparation of polyethylene reference materials with crystallinity about 90% [18], we found that there exists a distinguished difference crystallinity distribution within the skin layer and core region of cylindrical specimen crystallized under high pressure of 500–1000 MPa. To our knowledge, the 'skin-core' structure possessing different

---

* Corresponding author. Tel.: +86 29 88474139.
E-mail address: kongjie1976@hotmail.com (J. Kong).

0032-3861/$ - see front matter © 2005 Elsevier Ltd. All rights reserved.
doi:10.1016/j.polymer.2005.04.108

morphology and crystallinity has ever been investigated in the low-pressure injection-molded polypropylene [19,20], polyamide-6 [21] and poly (butylene terephthalate) [22]. And such structure is mainly controlled by the shear, flow and cooling conditions during the injection process. However, the visual characterizations of the 'skin-core' type of crystallinity distribution within the high pressure crystallized polyethylene are seldom reported, moreover, this 'skin-core' structure may exert great effect on the polyethylene based products fabricated under the high pressure crystallization process.

In this paper, the regularity of 'skin-core' type of crystallinity distribution within the cylindrical specimen of polyethylene crystallized under high pressure was investigated via modulated differential scanning calorimeter (MDSC), wide angle X-ray diffraction meter (WAXD), dynamic mechanical analyzer (DMA) and scanning electron microscope (SEM). And the proposed effect of gradient of the high pressure stress field on the 'skin-core' structure was also to be established in accordance with the basic high pressure crystallization theory of polymers. The study clearly indicated that the uneven distribution of high pressure stress field, especially, the high pressure decay effect at the edge of the plunger and cylindrical channel of the mold is the principal factor to the formation of the 'skin-core' type of crystallinity distribution within the polyethylene cylindrical specimen crystallized under high pressure.

2. Experimental

2.1. Materials

The high-density polyethylene (commercial brand: DMDY 1158) used in this study was from Qilu Petroleum and Chemical Corporation (Zibo City, Shandong Province, China). The physical parameters of the polyethylene were listed in Table 1. The molecular weight and molecular weight distribution were measured using a PL220 high temperature size exclusion chromatography (SEC, Shropshire, UK). 1,2,4-Trichlorobenzene was the elution solvent with a flow rate of 1.0 mL/min. The operating temperature was 160 °C. Polystyrene standards were used for making the calibration.

2.2. The preparation of specimen

Fig. 1 shows the scheme of a self-made crystallization apparatus that can load a high-pressure stress. The diameter of the plunger is 20 mm, and the length of the cylindrical channel is 200 mm. Hydrostatic pressure supplied is from a plastic molding machine, which is equipped with a modulated pressure meter having an auto-pressure compensator (Yuhua Rubber Machine Company, Xi'an, China). The magnitude of the pressure inside channel can be measured via the pressure meter, and the process temperature is controlled via a thermocouple mounted near the channel surrounded with a heating sheath. Before the experiment, the temperature of inside channel is carefully calibrated with the in-situ temperature measured by the thermocouple.

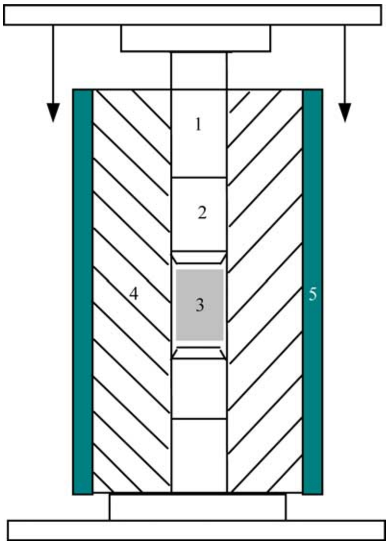

Fig. 1. The scheme of the high-pressure cell (1. Plunger; 2. Seal plunger; 3. Sample; 4. Mould; 5. Heater circle).

Specifically, 25 g of polyethylene resin was first put inside the channel of the mould, and heated to 230 °C. After keeping the temperature for 30 min, a predetermined pressure value of 650 MPa was applied to the melted resin during 2 min. Both the temperature and pressure for the system were kept for 10 min. Then the system is cooling to room temperature at a rate of 60 °C/h and release the pressure. The size of the cylindrical sample is 20 mm in diameter and 70 mm in high. And the specimens of polyethylene crystallized under high pressure and ambient pressure were labeled as HP-specimen and AP-specimen, respectively. In order to characterize the crystallinity distribution in longitudinal and latitude directions, the sampling locations in the two directions was shown as in Fig. 2(A) and (B), respectively.

2.3. Modulated differential scanning calorimeter (MDSC) analyses

A conventional differential scanning calorimeter (2910 MDSC, TA Instruments, New Castle, DE) equipped with

Table 1
Physical parameters of different density commercial polyethylene

Polyethylene	Density (g/cm^3)	$\bar{M}_w$	$\bar{M}_n$	$\bar{M}_w/\bar{M}_n$	Degree of SCB
DMDY1158	0.951∼0.955	281,000	23,000	12.0	12

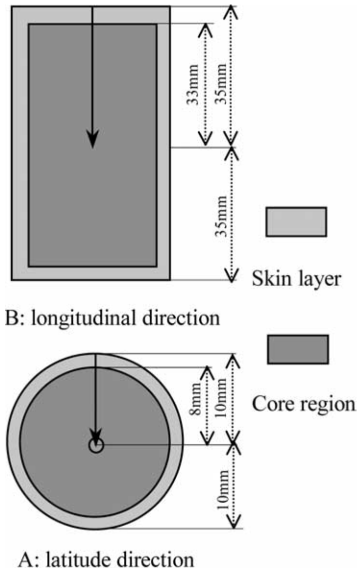

Fig. 2. Scheme of core region and skin layer the arrowhead representing the sampling.

refrigerated cooling system (RCS) was employed in the study. The temperature was calibrated with indium (156.6 °C) and the heat flow was calibrated with the specific heat of fusion of indium (28.71 J/g) at a scanning rate of 10 °C/min. The furnace was purged with dry nitrogen at a flow rate of 50 mL/min. About 5.0 mg sample was sealed in an aluminum pan, and the scanning procedure was conducted from −20 to 180 °C at a rate of 10 °C/min. The crystallinity was calculated by using the equation as follows [23,24].

$$X_c = \frac{\Delta H_u}{\Delta H_{100\%}} 100\%$$

where ΔH_u is the integrated melting enthalpy between 0 and 170 °C from DSC endothermic curve, $\Delta H_{100\%}$ is the melting enthalpy of polyethylene crystal with 100% crystallinity, which is set as 287.3 J/g in this study [25,26]. The lamella thickness (L^*) was calculated by using the Thomson–Gibbs equation as follows [27].

$$L^* = \frac{2\sigma_e T_m^0}{\mathit{\Delta} H_f(T_m^0 - T_m)}$$

where σ_e is side surface free energy, T_m^0 is the equilibriums melting point, T_m is the detected melting point by DSC, ΔH_f is melting enthalpy of unit volume polyethylene crystal. For the polyethylene in this study, σ_e, T_m^0 and ΔH_f were set as 90×10^{-3} J/m^2, 417.6 K and 287.3×10^6 J/m^3 [28].

A modulated differential scanning calorimeter (2910 MDSC, TA Instruments, New Castle, DE) was used equipping with refrigerated cooling system (RCS). The temperature was calibrated with indium (156.6 °C), and the heat flow rate was also calibrated with indium (28.71 J/g). The heat capacity constant was calibrated with sapphire. The scanning procedure was conducted from −40 to 180 °C at a rate of 5 °C/min with amplitude of ±0.5 °C in a period of 40 s.

2.4. Wide angle X-ray diffraction meter (WAXD) measurements

WAXD patterns of polyethylene samples were obtained with a Philips' WAXD diffraction meter (Philips, Netherlands) using Cu Kα as the radiation. The tube current and voltage are 40 mA and 40 kV, respectively. The measurement was scanned from 5 to 50° (2θ) at a rate of 2.5°/min at ambient temperature.

2.5. Dynamic mechanical analyzer (DMA) analyses

The dynamic mechanical properties for specimens were determined with a DMA instrument (Q800 DMA, TA instruments, New Castle, DE) using the film tensile mode. The testing procedure was conducted from −140 to 160 °C at a frequency of 5 Hz and a heating rate of 3 °C/min. The samples for measurements were cut from the cylindrical specimen with the size of $1.0 \times 5.0 \times 30$ mm^3.

2.6. Scanning electron microscope (SEM) inspection

The morphologies of the skin layer and core region were inspected by means of a scanning electron microscope (AMRAY model-1000B). The samples with very smooth surfaces were obtained from different locations of cylindrical specimen. Sample preparation was to use liquid nitrogen to freeze sample first, and then to cut them according to the desired size. The surface of samples was coated with golden before viewing.

3. Results and discussion

3.1. The regularity of crystallinity distribution within a cylindrical HP-specimen

The conventional DSC endothermic curves for slices of cylindrical HP-specimen obtaining in latitude and longitudinal directions are shown in Figs. 3 and 4, respectively. Evidently, there is only a single melting peak at 131 °C for samples from the skin layer, but for samples obtaining from the core region, there exist double melting peaks which may be attributed to the crystals with different thickness. The melting peak at 131 °C can be referred to the crystals with less perfection and lower crystallinity. The melting peak at 143.4 °C may be attributed to the more perfect crystals with relatively higher thickness and crystallinity. If utilize Hoffman–Weeks equation [26] to make a calculation, the average crystal thickness for the core region can reach as high as 210 nm, which is much higher than that for the skin layer with only 24 nm thickness. The analysis clearly suggests that the crystals from the core region may mainly consist of the extended chain crystals possessing higher crystallinity and higher melting point. Also as noticed in Figs. 3 and 4, the endothermic peaks gradually move to the

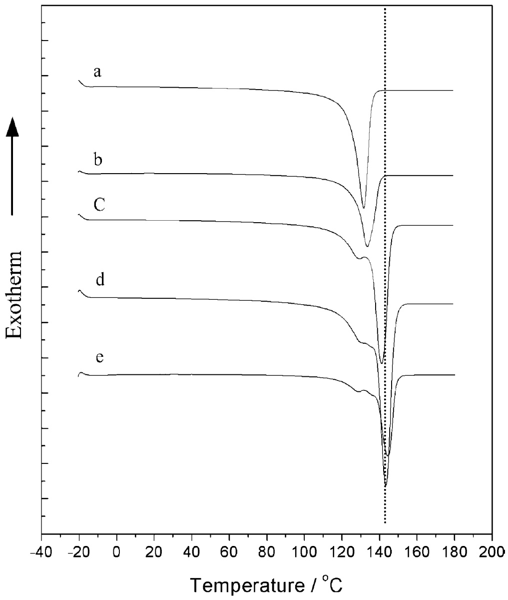

Fig. 3. The DSC curves of HP-specimen slices sampling from the latitude direction, the distance of slices from the surface for curve a, b, c, d and e are 0.1, 1.2, 2.0, 6.0 and 9.0 mm, respectively.

high temperature and the peak area increases accordingly following the change of sampling location. The results can be further observed in Figs. 5 and 6, where the crystallinity, and the melting point for polyethylene crystallized under the high-pressure are plotted with its sampling location. Clearly, the values of the crystallinity for the skin layer (within the edge of the samples about 2.0 mm) are from 73.2 to 74.5% with melting points from 131.5 to 132.4 °C, while the values of the crystallinity for the core region are basically the same around 90% with melting points from 141 to 144 °C. These data further confirm that, under the crystallization condition of high-pressure stress field, there exists indeed a marked difference both in crystallinity and the melting point between the skin layer and the core region within a cylindrical specimen of polyethylene crystallized under high pressure.

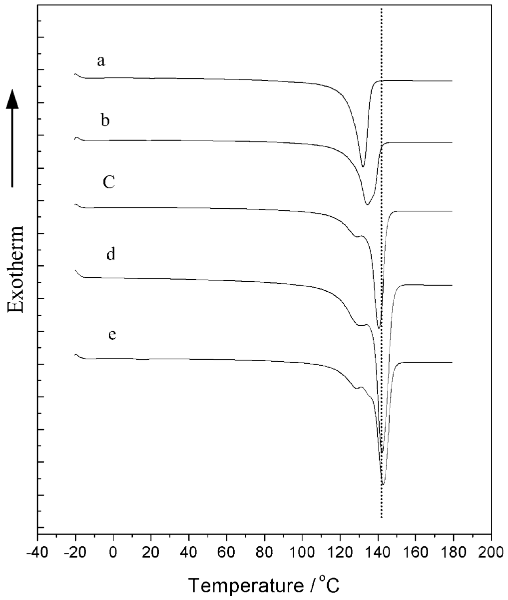

Fig. 4. The DSC curves of HP-specimen slices sampling from the longitudinal direction, the distance of slices from the surface for curve a, b, c, d and e are 0.1, 1.0, 2.0, 17.0 mm and 29.0 m, respectively.

3.2. The regularity of crystallinity distribution within a cylindrical AP-specimen

For comparison, we also conduct the crystallization process for polyethylene using the same equipment but under the ambient condition. The melting behaviors detected by DSC for samples from different locations according to Fig. 2 are presented in Figs. 7 and 8.

Obviously, there is only one single melting peak occurring for all samples, furthermore, no any difference for the melting point can be observed. The result indicates the sample's uniform structural character, thus there exists no 'skin-core' type of crystallinity distribution within the cylindrical specimen of polyethylene crystallized under ambient pressure. Interestingly, the values of the crystallinity and melting point of samples from the skin layer (within the edge of the samples about 1.5 mm) of HP-specimen are lower than that of the samples from the similar location of AP-specimen (see Figs. 5 and 6). The reduction values for the crystallinity and melting point are about 3%

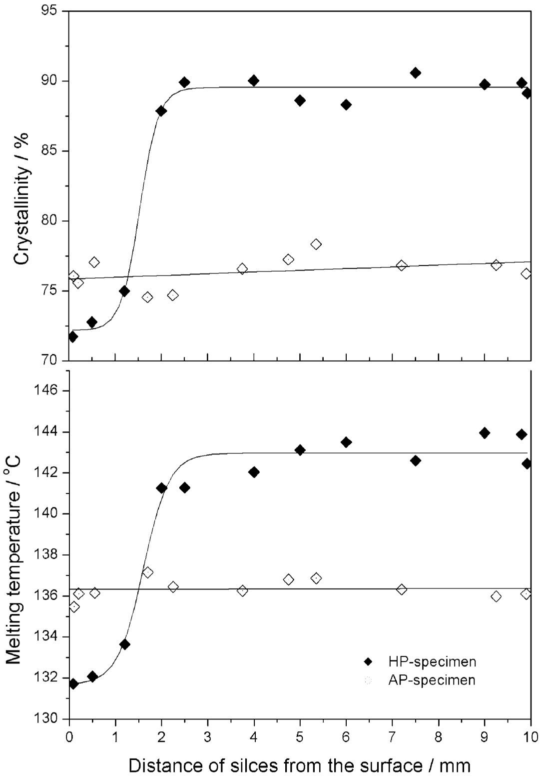

Fig. 5. The relationship between crystallinity, melting point and distance of slices from the surface in latitude direction for both HP-specimen and AP-specimen.

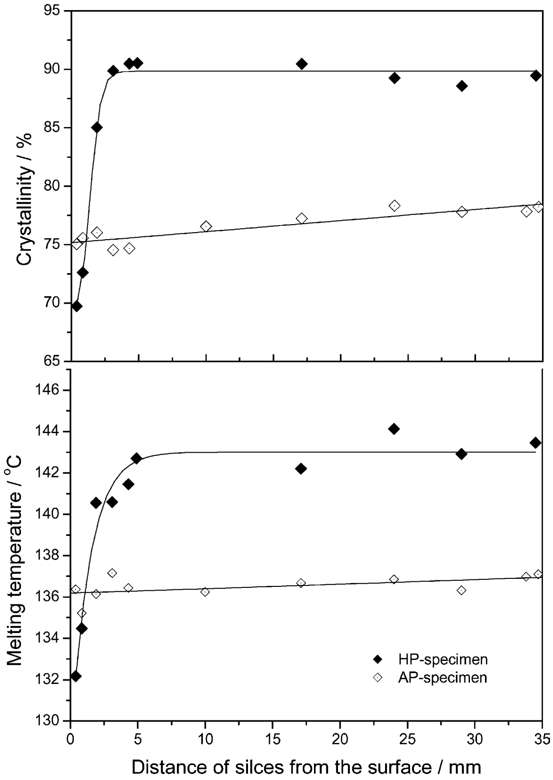

Fig. 6. The relationship between crystallinity, melting point and distance of slices from the surface in longitudinal direction for both HP-specimen and AP-specimen.

and 3 °C, respectively. As for the two crystallization processes, both the rates of temperature rising and cooling are basically the same, the crystallization for polyethylene under the high pressure stress field not only can produce the typical crystals with high crystallinity and high melting point, but also can cause lower the crystallinity near the skin layer, particularly, on the surface of the cylindrical specimen. The reason may be from the mechanism of the high pressure decay effect at the edge of plunger and cylindrical channel and a confined macromolecular movement by the wall of the model, as a result, reducing the extent of the macromolecular arrangement in three dimensional directions.

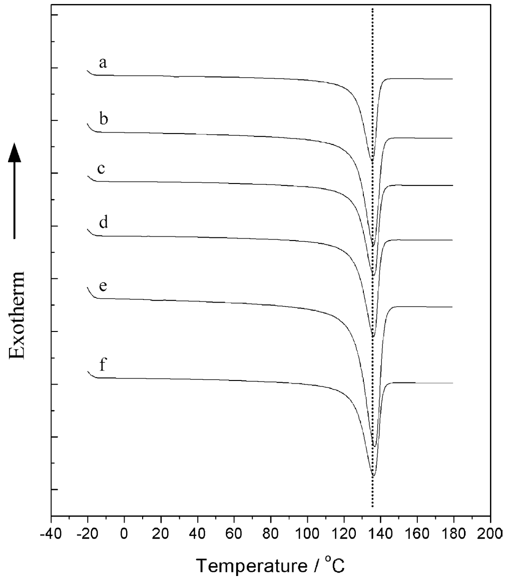

Fig. 7. The DSC curves of AP-specimen slices sampling from the latitude direction, the distance of slices from the surface for curve a, b, c, d, e and f are 0.1, 1.2, 2.0, 6.0, 8.0 and 9.0 mm, respectively.

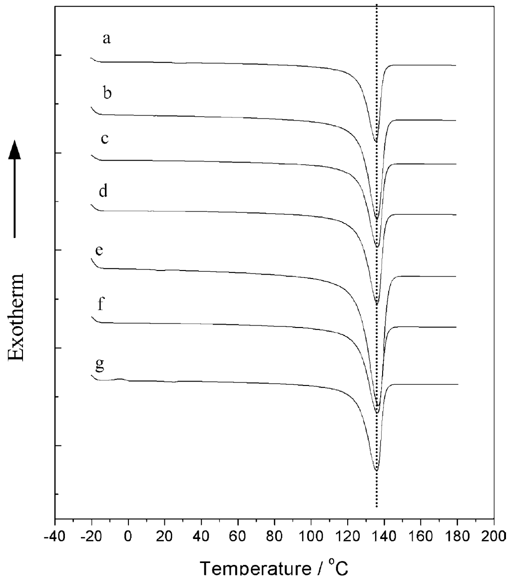

Fig. 8. The DSC curves of AP-specimen slices sampling from the longitudinal direction, the distance of slices from the surface for curve a, b, c, d, e, f and g are 0.1, 1.0, 2.0, 17.0, 20.0, 29.0 and 34.0 mm, respectively.

3.3. Analyses for skin layer and core region of HP-specimen

Modulated DSC is a technique that measures the difference of heat flow between a sample and a reference as a function of both time and temperature. A sinusoidal modulation (oscillation) is overlaid on the conventional linear heating ramp to yield a profile in which the average sample temperature continuously changes with time but not in a linear way. The total heat flow of MDSC, which is the only heat flow measured by conventional DSC, is composed of two components: the reversible and non-reversible heat flows. The former is a function of the sample's heat capacity and heating rate, and the latter is the heat flow related to the kinetic process [29,30]. Thus, with two components, especially from the non-reversible heat flow, one can detect and understand the degree of perfection of polyethylene's crystalline structures [31]. The MDSC curves of reversible, non-reversible and the total heat flows for skin layer and core region of the polyethylene crystallized under high pressure are shown in Fig. 9.

As can be seen, although all MDSC curves possess a sharp endothermic peak, there exists marked difference for the two different samples. For the skin layer, there is only a single lower melting point for three heat models, which may be from the melting of the folded chain crystals. But for the core region, the curves of reversible, non-reversible and total heat flows all present a main endothermic melting peak and a small shoulder peak. It reveals the existence of two kinds of crystals with different thickness. However, the value of reversible thermal enthalpy is nearly equal for both skin layer and core region samples, while the value of non-reversible thermal enthalpy for core region is much higher than that of skin layer. Considering reversible thermal enthalpy is related to the thermal capacity, but the non-reversible thermal enthalpy is related to the kinetic processes of melting, the higher non-reversible thermal enthalpy implies that macromolecules in core region experience a much strong forced crystallization process. It is this crystallization process that leads to the occurrence of high non-reversible thermal enthalpy in MDSC curves. On the other hand, duo to the existence of uneven distribution of high pressure stress field as well as pressure decay effect at the edge of plunger and cylindrical channel of mold, the skin layer is not greatly affected by high-pressure stress field, as a result, the lower non-reversible thermal enthalpy is observed. The results of MDSC again demonstrate that the pressure is the principal factor to cause the 'skin-core' type of crystallinity distribution within HP-specimen.

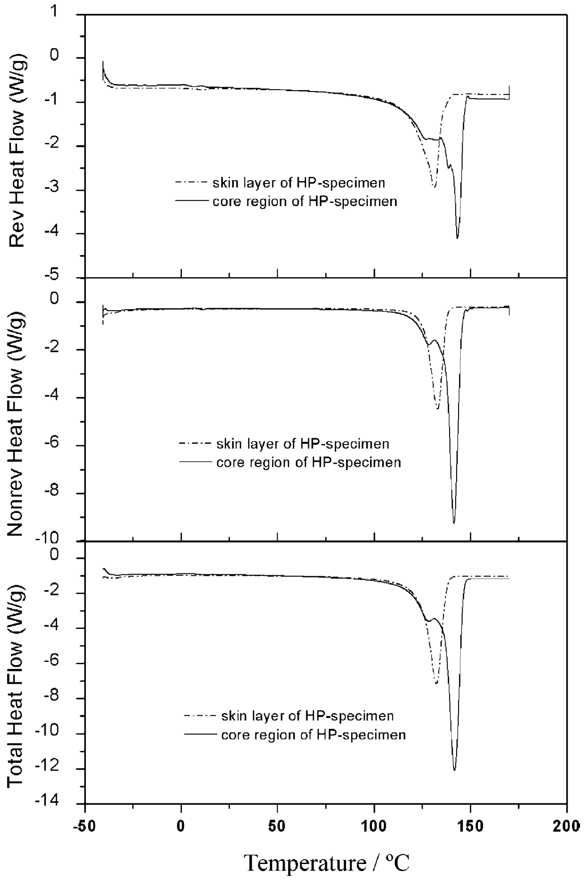

Fig. 9. The MDSC thermograms of skin layer and core region of HP-specimen.

3.4. WAXD analyses for skin layer and core region of HP-specimen

Wide-angle X-ray diffraction patterns for the skin layer and the core region of polyethylene specimen crystallized under high pressure are presented in Fig. 10.

Evidently, the diffraction intensity of crystallographic planes (110) and (200) for the core region sample is higher than that of the skin region sample. On the contrary, the diffraction intensity of dispersion planes is lower. It clearly indicates the crystals in the core region were well developed, and the overall crystallinity of the core region is higher than that of the skin region, which is corresponding to the results from the DSC and MDSC measurements. Moreover, the peak position of the crystallographic planes (110) and (200) for core region shift to larger angle in some sort. The result reveals the crystals with little lattice constant are packing in the core region of the polyethylene specimens crystallized under high pressure.

3.5. DMA analyses for skin layer and core region of HP-specimen

The spectra of thermal dynamic mechanical analyses for the skin layer and the core region samples of polyethylene specimen crystallized under high pressure are presented in Fig. 11.

As can be seen from the curves of storage modules, the value for the core region sample is much higher than that of the skin layer sample in a wide temperature range. The result reflects that the core region samples possess much higher stiffness and rigid which can be attributed mainly to its higher crystallinity. On the other hand, the curves of loss modules for both samples show two relaxation peaks at the temperature of −110 and 60 °C, respectively. It is well known that, for high-density polyethylene, the relaxation peak at −110 °C is associated with small segment's crankshaft movement in the amorphous region. The relaxation peak at 60 °C is from the movement of crystalline

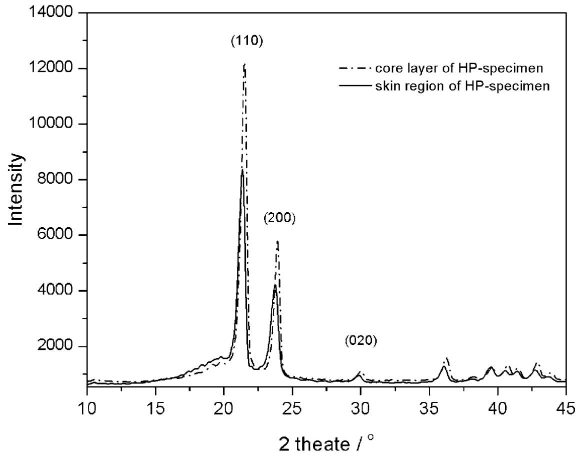

Fig. 10. WAXD curves of skin layer and core region of HP-specimen.

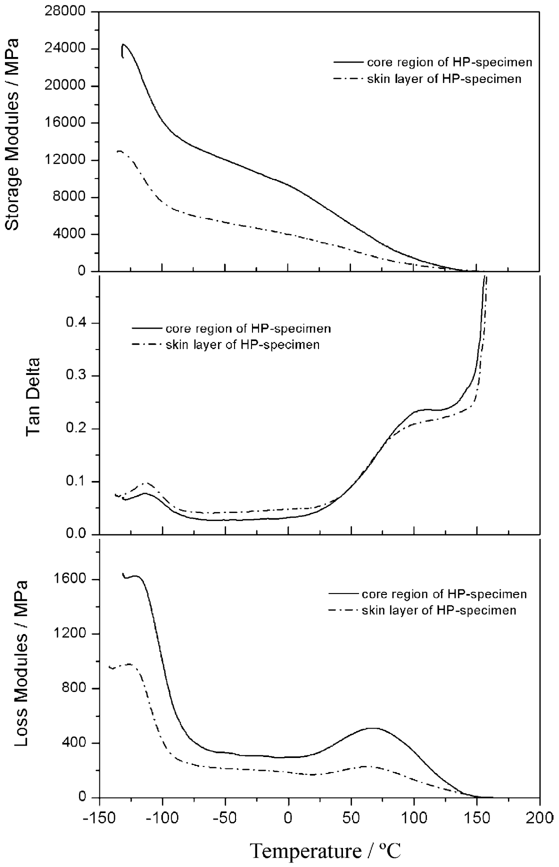

Fig. 11. DMA curves of skin layer and core region of HP-specimen.

phase, which is usually described as a complex multi-relaxation process consisting of α and α', types of relaxation [32]. α relaxation can be attributed to the movement of chain segments in the lamellar crystals plane, and folded surface or cilia between lamellar crystals. And α' relaxation is from the inter-lamellar sliding of crystals at the higher temperature. Usually the increase in the intensity of α relaxation peak is connected with a high crystallinity in polyethylene [33,34]. In this study, the intensity of α relaxation peak of the core region sample is obviously larger than that of the skin layer sample. And the relaxation peak also shifts to the higher temperature. Therefore, DMA data further prove that there exists higher crystallinity and larger thickness crystals in the samples from the core region. In addition, as can be seen from the curves of tan δ, compared with the skin layer, the intensity of low temperature relaxation peaks (below -110 °C) for the core region decreases, and the peak position also shifts to a higher temperature revealing the similar results obtaining from storage modules and loss modules measurement.

3.6. Morphological inspections of skin layer and core region of HP-specimen

The SEM images of the fracture surface for skin layer and core region of polyethylene specimen crystallized under high pressure are shown in Fig. 12.

Evidently, the surface of the skin layer presents a relatively smooth morphology, and many striations with high tacticity are presented in the SEM photo for core region. This is suggested that there mainly exist marked difference of morphology between the skin layer and core region of polyethylene specimen crystallized under high pressure.

3.7. The effect of gradient of high pressure stress field on the 'skin-core' structure of HP-specimen

As is confirmed above, there exists the 'skin-core' type of crystallinity distribution within polyethylene specimen crystallized under high pressure. In some respects, the results may be similar with the reported 'skin-core' structure in low pressure injection-molded polymers such as polypropylene [19,20], polyimide-6 [21], poly (butylene terephthalate) [22], and the oxygen plasma treated HDPE sample [35], which is mainly controlled by the shear, flow, cooling conditions during the injection process and plasma treatment. The main reason may be from the existence of gradient of high-pressure stress filed. According to the principal of hydrodynamics, before cooling, the high-pressure stress should be distributed uniformly onto polyethylene melt [9,13]. However, as the melt is subjected to cooling under the high pressure, its phase transformation occurs inevitably. On the other hand as the rapid cooling rate near the wall of the mold and causing the pressure decay at the edge of plunger and cylindrical channel, the phase transformation in the melt becomes uneven. The uneven distribution of high-pressure stress field, particularly lower near the skin layer and higher around core region, is formed. Consequently, the polyethylene melt may be subjected the different pressure strength in accordance with the different locations. Around the core region, the crystallization carries out under the high pressure and high temperature, as a result, the macromolecules can easily slide and diffuse along the chain axes direction, and form the extended chain crystals with higher thickness and higher crystallinity according to the 'chain slide and diffuse theory' [36-38]. For the skin layer, however, the crystallization conducts under a relatively lower pressure due to the stress decay effect, accordingly, the macromolecules may form folded chain lamellar crystals with lower crystallinity that has been already proved via DSC, WAXD analysis and morphological inspections. Thus the 'skin-core' type of crystallinity distribution is formed within polyethylene specimen crystallized under high pressure.

4. Conclusions

In conclusion, it is found that there exists a distinguished feature of a 'skin-core' type of crystallinity distribution within the cylindrical specimen of polyethylene crystallized

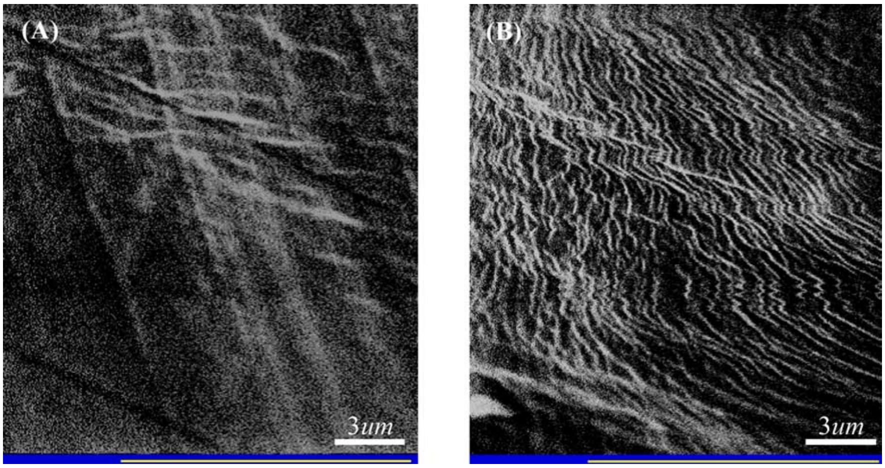

Fig. 12. SEM images of skin layer and core region of HP-specimen (A) skin layer; (B) core region.

under the high pressure. The specimen's core region consists of the extended chain crystals with higher crystallinity and higher melting point; however the specimen's skin layer consists of folded chain crystals with lower crystallinity and lower melting point. The measurement data of the non-reversible heat flow of MDSC and WAXD for both skin layer and core region are in accordance with that marked difference. Especially, the MDSC analyses reveal that the difference of crystallinity between the skin layer and core region could reflect in their non-reversible thermal enthalpy. Based on the law of stress decay of high pressure field and the 'chain slide and diffuse' high pressure crystallization theory of polyethylene, it was found that the uneven distribution of high pressure stress field, that is, the high pressure decay effect at the edge of plunger and the cylindrical channel of mold is the principal factor to cause the 'skin-core' type of crystallinity distribution.

Acknowledgements

This study was financially supported by a Meterage Foundation Project (contract grant number: 61005217), from the National Defense Ministry of China.

References

[1] Bassett DC. Polymer 1976;17(6):460–70.

[2] Takeshi, Hattori, Masamichi, Hikoska, Hiroji, Ohigashi. Polymer 1996;37(1):85–91.

[3] Siegmann A, Hargect PJ. J Polym Sci, Part B: Polym Phys Ed 1980; 18(11):2181–96.

[4] Liangbin Li, Chunmei Wang, Rui Huang, Ling Zhang, Shiming Hong. Polymer 2001;42:8867–72.

[5] Wunderlich B. J Polym Sci: Part A-2 1963;1:1245–62.

[6] Geil PH, Anderson FR, Wunderlich B, Arakawa T. J Polym Sci: Part A-2 1964;6707.

[7] Annis BK, Reffiner JR, Wunderlich B. J Polym Sci, Part B: Polym Phys 1993;31(1):93–7.

[8] Jackson JF, Hsu TS, Brasch JW. J Polym Sci, Part B: Polym Phys 1972;10(3):207–24.

[9] Qiang Fu, Rui Huang. Chin Sci Bull 1995;40(20):1909–12.

[10] Shaoxian Peng, Rui Huang, Bihua Cai, Banghu Xie. Chin Prog Sci 1997;7(1):35–40.

[11] Nakafuku C, Nishimura K. J Appl Polym Sci 2003;87(12):1962–8.

[12] Hosier IL, Bassett DC. Polymer 2002;43(22):5979–84.

[13] Qiang Fu, Rui Huang, Xiongwei Zhang. Sci China: E 1996;26(5): 467–73.

[14] Flores A, Baltacalleja FJ, Bassett DC. J Polym Sci, Part B: Polym Phys 1999;37:3151–8.

[15] Guan Q, Zhu X, Chiu D, Shen K, Lai FS, McCarthy SP. J Appl Polym Sci 1996;62:755–62.

[16] Kubat J, Manson JA, Rigdahl M. Polym Eng Sci 1983;23:877–85.

[17] Maxwell AS, Unwin AP, Ward IM. Polymer 1996;37(15):3283–91.

[18] Jie Kong, Xiaodong Fan, Yunchuan Xie, Wenqiang Qiao. Chin Polym Mater Sci Eng 2004;20(5):178–81.

[19] Trotignon JP, Verdu J. J Appl Polym Sci 1990;39(5):1215–7.

[20] Wenig W, Herzog F. J Appl Polym Sci 1993;50(12):2163–71.

[21] Murthy NS, Kagan VA, Bray RG. Polym Eng Sci 2002;42(5):940–50.

[22] Hobbs SY, Pratt CF. J Appl Polym Sci 1975;19(6):1701–22.

[23] Jie Kong, Xioadong Kong, Mei Jia. J Appl Polym Sci 2004;93(6): 2542–9.

[24] Kong Y, Hay JN. Polymer 2002;43(14):3873–8.

[25] Wunderlich B, Cormier CM. J Polym Sci: Part A-2 1967;5:987–8.

[26] Jie Kong, Xiaodong Fan, Yunchuan Xie, Wenqiang Qiao. J Appl Polym Sci 2004;94(4):1710–8.

[27] Darras O, Seguela R. Polymer 1993;34:2946–50.

[28] Hoffman JD. Polymer 1997;38(13):3151–212.

[29] Reading M, Elliott D, Hill VL. J Therm Anal 1993;40:949–55.

[30] Gill PS, Sauerbrern SR, Reading M. J Therm Anal 1993;40:931–9.

[31] Yunchuan Xie, Qian Zhang, Xiaodong Fan. J Appl Polym Sci 2003; 89:2686–91.

[32] QianG B, Xu G, Yu F. Transition and relaxation of polymer. Chinese Science Press; 1986 p. 336.

[33] Pakula T, Kryszewski M, Pluta M. Eur Polym J 1977;13:141–8.

[34] Kyu T, Suehiro S, Nomura S, Kawai H. J Polym Sci, Part B: Polym Phys Ed 1980;18:951–70.

[35] Indranil B, Kwang SK, Yo IY, Dae HK, Chang MR, Chan SP, et al. Polymer 2003;44(4):1163–70.

[36] Hikosaka M. Polymer 1987;28:1257–64.

[37] Hikosaka M. Polymer 1990;31:458–68.

[38] Hikosaka M, Amano K, Rastogl S, Kwller A. Macromolecules 1997; 30:2067–74.